Structural and Thermal Characterization of Mono- and Diacyl Polyoxyethylene Glycol by Infrared Spectroscopy and X-ray Diffraction Coupled to Differential Calorimetry

J. B. Brubach,*,† M. Ollivon,† V. Jannin,‡ B. Mahler,‡ C. Bourgaux,§ P. Lesieur,§ and P. Roy§

Laboratoire de Physicochimie des Systèmes Polyphasés, UMR 8612, Faculté de Pharmacie, 92296 Chatenay Malabry, France, Gattefossé S. A. S., BP 603 69804, Saint-Priest Cedex, France, and LURE, Université Paris Sud, 91405 Orsay Cedex, France

Received: May 11, 2004; In Final Form: August 10, 2004

Physical and thermal properties of polyoxyethylene glycol glycerides (Gelucire 50/13) used as sustained-release matrix forming agent in pharmaceutical applications are studied by coupled time-resolved synchrotron X-ray diffraction and differential scanning calorimetry combined with infrared spectroscopy. With these techniques, all polymorphs formed after various thermal treatments from quenching to slow crystallization are characterized. In particular, the fatty esters of polyoxyethylene glycol (PEG) polymorph conformations are all provided by the same lamellar phase with the PEG chains under a helical conformation but with a more or less important tilt of the PEG chains. The rate of crystallization was crucial for the formation of these polymorphs. A slow crystallization rate (0.1 °C/min) will induce the formation of a 120 Å lamellar phase presenting a higher melting point and consequently a better stability in time and in temperature. Inversely, a rapid crystallization rate will induce the formation of a 90 Å lamellar phase. We show, however, the possibility of a rapid transition toward the most stable form. Possible interdigitation of fatty acid chains is also discussed.

I. Introduction

Semisolid matrixes are often used in the composition of hard gelatin capsule formulations for modified drug release. The choice of excipient depends on the type of drug and also on the profile of release required.[1−3] Such excipient is frequently made from lipids and for this reason an important variety of excipient is available. Gelucire 50/13 (the two numbers correspond, respectively, to the drop point and the hydrophilic−lipophilic balance value or HLB) consists of a mix of mono-, di-, triacyl glycerol (around 20% in weight) and monoacyl polyoxyethylene glycols and diacyl polyoxyethylene glycols labeled, respectively, MPEG and DPEG. These compounds have several capabilities, including drug encapsulation whether the drug's form is liquid or solid and foremost it allows the control of the drug release. In fact, by changing the melting point and the HLB value used as a measure of the polarity of the surface-active molecule, the amount of drug released per unit of time can be controlled.[4] As drug release depends on the stability of the crystalline structures formed, it is of prime importance to characterize any possible structural evolution of the excipient. Therefore, a description of these various phases is necessary both for the pharmaceutical science as it is linked to drug and excipient polymorphism and for a more general understanding of the chemistry of this family of systems.

The first objective of this study is to evidence all possible polymorphs of Gelucire 50/13 and second to control the formation of these polymorphs under particular experimental conditions. For example, understanding the thermal and structural variations of these compounds with time might allow us to prevent it by an adequate thermal treatment.

Glycerides and polyoxyethylene glycol (PEG) are subject to an extensive literature including a variety of experimental[5−9] and theoretical tools and models derived from computational results based on molecular simulation.[10,11] In this study, the polymorphic evolution of glycerides and mono- and diacyl polyoxyethylene glycols has been characterized by the combined use of coupled X-ray diffraction and differential scanning calorimetry[12] and infrared spectroscopy. X-ray diffraction allows the study of the structure and the polymorphism of the lipid compounds. WAXS region corresponds to short reticular distances between hydrocarbon chains while SAXS domain corresponds to long spacing. DSC, by temperature and enthalpy of transition measurement, highlights energetic phenomena that occur during the heating or the cooling of the sample. By coupling these two techniques, we can link structural changes to phase transitions. Infrared spectroscopy is a complementary technique to the X-ray diffraction and has also been intensively used to determine chain positioning and conformation of glycerides and PEG at the molecular level.[13,14,15]

The aim of this study is to present, as a function of temperature and thermal history of the sample, a complete structural representation of Gelucire 50/13 in particular at the molecular scale of PEG chains. For this purpose, structural and thermal studies were performed on free PEG 1500 which is the main constituent used for the synthesis of the Gelucire 50/13. This structural analysis will be used to separate the contribution provided by the glycerides part and this given by the polyoxyethylene glycol part.

II. Materials and Methods

Small pellets of Gelucire 50/13 and poly(ethylene glycol) of average molecular weight 1500 (PEG 1500) were supplied by

* Author to whom correspondence should be addressed. E-mail: Jeanblaise.brubach@cep.u-psud.fr.
† Laboratoire de Physicochimie des systèmes polyphasés.
‡ Gattefossé S. A. S.
§ Université Paris Sud.

10.1021/jp047989m CCC: $27.50
Published on Web 10/21/2004

Gattefossé S. A. S., St Priest (France), and were analyzed without any special thermal treatment (as received). Gelucire 50/13 is synthesized by an alcoholysis/esterification reaction using as starting materials hydrogenated palm oil and PEG 1500, equivalent to approximately 34 monomer units −CH2−CH2−O−, and ended by two alcohol groups. Gelucire 50/13 is a mixture of mono-, di-, and triglycerides and mono-, diacyl polyoxyethylene glycols. For glycerides mixture (approximately 20% in weight of the sample), the predominant fatty acids chains is the palmitostearic acid (C_{16} and C_{18}), with approximately the same proportion of mono-, di-, and triglycerides. However, the main part of the sample is composed of mono- and diacyl polyoxyethylene glycols (72% in weight) corresponding, respectively, to PEG 1500 ended by one or two acyl chain (in C_{16} or C_{18}). Chemical analysis performed on this sample has shown a proportion of 43% of DPEG and 29% of MPEG. The 8% remaining is free PEG 1500.

X-ray diffraction measurements were performed at the D22 and D24 beam line of the synchrotron ring storage LURE-DCI, University of Paris Sud, Orsay, France. On these two experimental setups, X-ray diffraction pattern and DSC were collected simultaneously. The high resolution, high flux, and long distance (up to 3 m) between the sample and the detector of D24 allow to investigate a large range of scattering vectors with a linear response, which in turn permits access to scattering vectors compatible with the longest structure. Therefore, all the SAXS patterns were recorded on this setup. The D22 beam line allows high quality recording with low noise; moreover, SAXS, WAXS, and DSC experiments can be performed simultaneously. The position sensitive linear detectors of SAXS and WAXS were calibrated, respectively, with silver behenate and tristearin (SSS).

The IR transmission spectra of the sample were recorded using a Bomem DA8 Fourier transform spectrometer, under vacuum, at the SIRLOIN beam line[16−18] at super-Aco synchrotron ring, LURE, University of Paris Sud, Orsay France. The mid-infrared region (500−9000 cm^{-1}) was investigated thanks to a globar source, in combination with a KBr beam splitter and an MCT wide range detector. Spectra were recorded with a resolution of 2 cm^{-1} with 200 scans per spectrum and no mathematical correction (e.g., smoothing) was performed. Transmission measurements of both reference and sample were performed using a variable path cell equipped with two 0.5-mm-thick diamond windows.

III. Results and Discussion

III.1. Structural and Thermal Studies of PEG1500. This section presents the results of SAXS, WAXS, and DSC experiments obtained simultaneously on a sample of PEG 1500. The 3D evolutions of SAXS and WAXS intensity versus scattering vector q upon heating are depicted in Figures 1 and 2. For each X-ray pattern, mathematical treatments were performed to determine position, maximum intensity, and half width at middle height of each X-ray diffraction peak. The lower part of each figure shows the evolution of X-ray diffraction peak positions (d(Å)) as a function of temperature. For all SAXS and WAXS analysis, the size of the symbol is proportional to the maximum of intensity of the peak. The DSC curve is superimposed on these results and consequently we can link thermal events to phase transitions or structural changes.

In Figure 1 at $T = 20$ °C, SAXS patterns show three sharp peaks: 0.064 $Å^{-1}$, 0.128 $Å^{-1}$, and 0.189 $Å^{-1}$ (d(Å) = (2*pi)/q($Å^{-1}$) = 96.7, 49.0, and 33.2 Å). They can be ascribed, respectively, to the first, second, and third order of a single lamellar phase with a long period of 96.7 Å. Simultaneously, WAXS patterns show two strong peaks at 1.35 $Å^{-1}$ and 1.64 $Å^{-1}$ and several minor peaks at 1.07 $Å^{-1}$, 1.31 $Å^{-1}$, 1.48 $Å^{-1}$, 1.55 $Å^{-1}$, and 1.89 $Å^{-1}$.

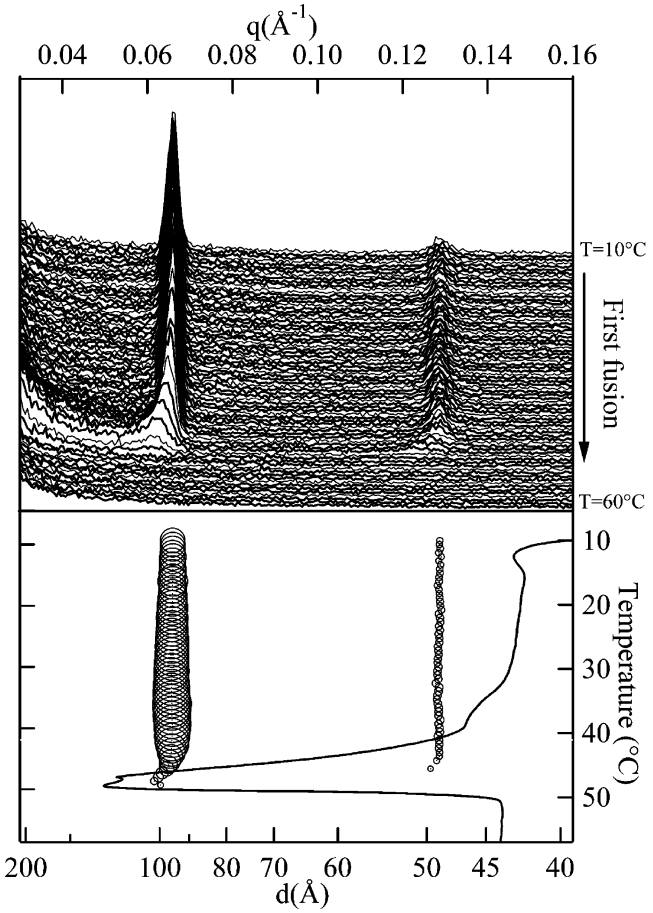

Figure 1. Evolution of SAXS patterns with the temperature for the first fusion of a sample of PEG 1500. The third order at d(Å) = 33.2 Å is not shown.

Until the temperature reaches 32 °C, the peak at 0.065 $Å^{-1}$ presents an important and gradual increase of intensity (64%), whereas the peak width at half-maximum and the position of the maximum of the peak stay constant. Moreover, no drastic change is observed, except a slight shift of the two bands at 1.35 $Å^{-1}$ and 1.636 $Å^{-1}$ to smaller q values. This can be related to DSC evolution where an endothermic phenomenon occurs at $T_{onset} = 31$ °C. Such evolution could be explained by the semicrystalline structure of the sample, which contains both crystalline and amorphous regions.[11] With the increase of temperature, the proportion of crystalline phase rises up to the detriment of the amorphous phase.

Beyond 39 °C, the melting of the sample is observed simultaneously in SAXS and WAXS where a rapid decrease of all peaks intensity occurs. At the same time, a marked shift toward low q values is observed in SAXS for the peak at 0.065 $Å^{-1}$ passing from 0.0658 $Å^{-1}$ (95.5 Å) to 0.0616 $Å^{-1}$ (102.0 Å) at $T = 48$ °C. This shift is accompanied by a dramatic increase of the scattering at lower q (Figure 1). Simultaneously, DSC signal shows two thermal events superimposed which can be linked to these structural changes.

WAXS patterns are directly related to the lateral organization of the molecules and depend on the chain packing subcell adopted. Previous studies[19−21] have already observed such diffraction peaks and several structures have been proposed.

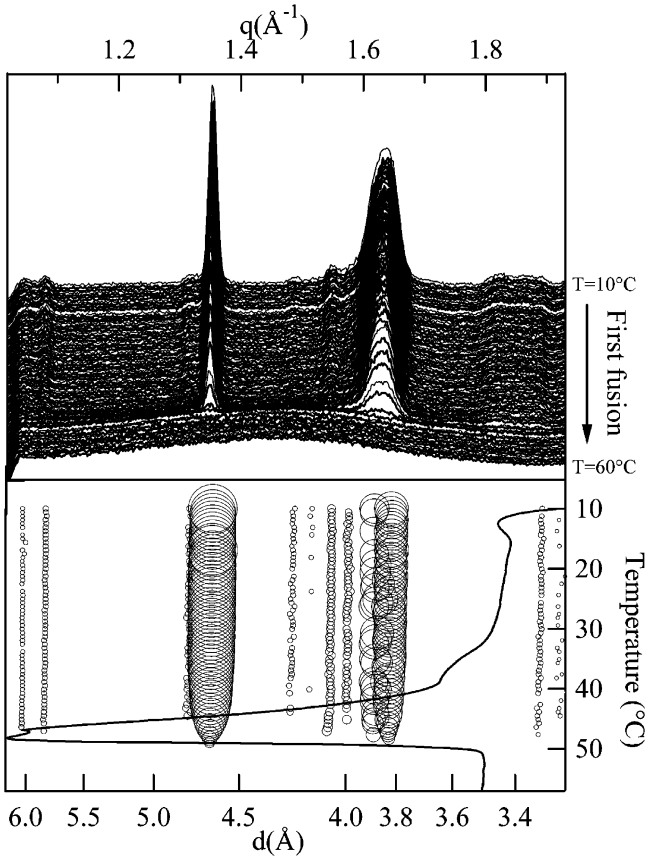

Figure 2. Evolution of WAXS patterns with the temperature for the first fusion of a sample of PEG 1500.

Evans et al.[21] and Takahashi et al.[22] have observed a zigzag conformation. In this case, the fiber period is 7.12 Å for two ethylene oxide (EO) units under tension. Takahashi et al.[5,23] and Neyertz et al.[10] have shown that PEG can also crystallize in a slightly distorted helical structure noted (7/2) helix. In that case, crystalline PEG is monoclinic and the cell parameters are $a = 8.05$ Å, $b = 13.04$ Å, $c = 19.48$ Å (fiber axis), and beta = 125.4°. This unit cell contains two left- and two right-handed helical chains, each containing seven $-(CH_2-CH_2-O)-$ monomer units. A value of 2.78 Å per monomer along the chain axis is found in such a conformation.

Further insight of the PEG chain conformations can be gained by comparing the diffraction pattern of PEG 1500 to simulated X-ray pattern, generated from the cell and the atomic parameters of the planar zigzag and the helical conformation.[5,22] Figure 3 displays the comparison between WAXS pattern obtained for PEG 1500 and generated by the software (Carine crystallographic 3.1) for a helical conformation. The strong similarity between the two curves clearly suggests that PEG 1500 adopts such a helical conformation.

For the SAXS domain, however, the simulated pattern is not in good agreement with the measurements. A difference of 17.2 Å is found between the period of the SAXS pattern of the PEG 1500 (96.7 Å) and the simulated one (79.5 Å). Changing the tilt of the PEG chains can reduce the gap between these two values. Passing from a monoclinic subcell to an orthorhombic subcell ($\alpha = \beta = \gamma = 90°$) leads to an increase of the long period of the lamellar phase. In this case, a theoretical length of 93.7 Å is found for PEG chains without tilt which is close to the value of 96.7 Å found on our sample (see Table 1). The remaining difference may be explained by the uncertainty on the distance between the two hydroxyl groups of the PEG.

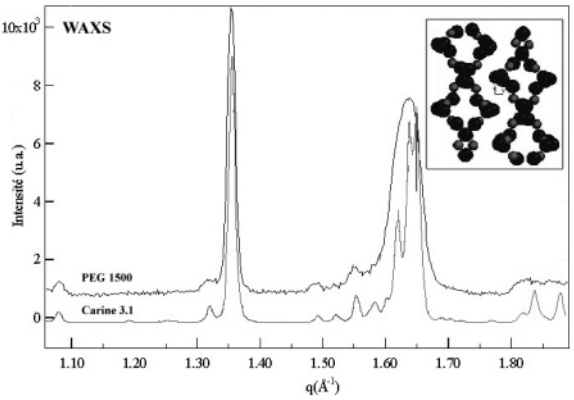

Figure 3. Comparison between WAXS pattern for PEG 1500 and the simulated X-ray pattern obtained using Carine 3.1 for a helical conformation of PEG chains, $T = 20$ °C.

TABLE 1: Comparison of the Different Long Periods Observed for PEG 1500 by X-ray Diffraction and Generated by the Software Carine Crystallography 3.1

techniques		long period	tilt angle
experimental	X-ray diffraction	96.7 Å	
theory	monoclinic subcell	79.5 Å	$\beta = 125.4°$
	orthorhombic subcell	93.7 Å	$\beta = 90°$

The comparison with simulated X-ray pattern suggests that at room temperature PEG 1500 forms a lamellar phase with a long spacing of 96.7 Å. It corresponds to an organization of the PEG chains under a helical conformation with an orthorhombic subcell. The lack of change in the structure with the temperature suggests that there is a single lamellar phase in the crystallized phase of PEG 1500.

III.2. Structural Study of Gelucire 50/13. *A. SAXS Studies.* Figure 4a, c, and e represents the SAXS 3D evolution of untreated Gelucire 50/13 during the cycle of fusion−crystallization−fusion between 20 °C and 60 °C with a heating rate of 1 °C/min. Figure 4b, d, and f represents the evolution of the position and the intensity (size of the symbols) of each peak observed in SAXS. The domain of q(Å^{-1}) covered is ranging from 0.02 Å^{-1} to 0.16 Å^{-1}.

At $T = 20$ °C, three lamellar phases with different long spacing periods are observed. Therefore, one can observe a first lamellar phase with Bragg reflections in the positional ratio 1:2:3 corresponding to q(Å^{-1}) values at 0.051 Å^{-1}, 0.10 Å^{-1}, and 0.152 Å^{-1} (respectively, 121, 62.5, and 41.3 Å). A second lamellar phase characterized by reflection in the positional ratio 1:2 is also observed for q(Å^{-1}) equal to 0.07 Å^{-1} and 0.14 Å^{-1} (90 and 45 Å). For these two structures, no changes in position and width are observed until the temperature reaches 35 °C for which the lamellar phase of 121 Å presents an important decrease of the peak width at middle height and a gradual increase in intensity which reaches a maximum at $T = 42$ °C. Simultaneously, the first-order reflection peak at 0.07 Å^{-1} decreases drastically in intensity and completely disappears. The presence of an isobestic point (at about $q = 0.06$ Å^{-1}) and the equal but opposite variation of the intensity of the two peaks (18% at $T = 42$ °C) shows clearly equilibrium between these two structures (0.072 Å^{-1} and 0.051 Å^{-1}) with temperature. This transition corresponds to the change of sign of the first derivative of the DSC peak. In fact, the melting of the first structure likely leads to an exothermic peak that superimposes to the endotherm as the sharp peak observed on Figure 4b. Only the resulting thermal event is observed. Above 42 °C, the lamellar phase of 121 Å gradually melts; this phenomenon corresponds to a second endothermic event.

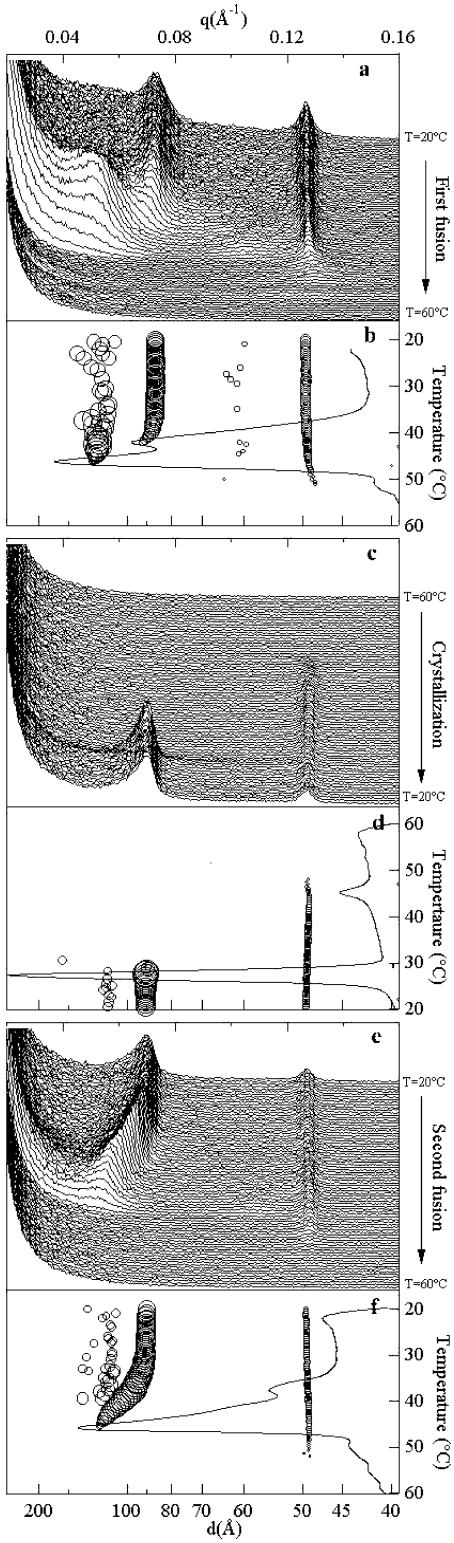

Figure 4. Evolution of SAXS patterns with the temperature for (a) the first fusion, (c) the crystallization, and (e) the second fusion of the untreated sample of Gelucire 50/13 at 1 °C/min. (b, d, f) Position and intensity (size of the symbol) of each peak observed in SAXS.

A third lamellar structure is observed at 0.127 $Å^{-1}$ (49.5 Å). This phase presents no important modification as the temperature is increased and is not linked to the former phases. Furthermore, this phase is the last one to melt above 54 °C and is related to the small endothermic event present at $T_{onset} = 50$ °C.

Moreover, as shown by the crystallization of the sample (see Figure 4c−d), the same structure crystallizes at 47 °C whereas the two other lamellar phases at 0.055 $Å^{-1}$ and 0.070 $Å^{-1}$ only crystallize at 29 °C. The lag time observed between crystallization and melting temperatures is important. This lag time was related to the metastability of the variety formed upon crystallization.

During the second fusion (Figure 4e−f), the same structures are observed. For the peak at 0.127 $Å^{-1}$, no changes in position, intensity, or width are observed. However, the temperature evolutions of the two lamellar phases of 121 and 90 Å are clearly different than the first fusion. In fact, inversely at 20 °C the lamellar phase of 90 Å is predominant in proportion and only a small shoulder is observed for the lamellar phase of 121 Å. Above 33 °C, the intensity of the peak at 0.07 $Å^{-1}$ increases by more than 50% and reaches a maximum at 35 °C. The same phenomenon was previously observed for the PEG 1500 and was attributed to the increase of the crystalline phases at the expense of the amorphous phase. Simultaneously, no change in line width is observed but the peak position shifts toward low q values ($T = 39$ °C, 0.065 $Å^{-1}$ or 97 Å). Two endothermic events occur in succession at $T_{onset} = 32$ °C and $T_{onset} = 37$ °C. They were attributed, respectively, to the increase of the intensity and the shift toward low q values of the same peak. Finally, above 40 °C, the intensity of the SAXS peak decreases continuously and the peak position shifts until reaching 0.052 $Å^{-1}$ before vanishing.

B. WAXS Measurements. Figure 5 represents the WAXS 3D evolution of untreated Gelucire 50/13 during the cycle of fusion−crystallization−fusion between 20 °C and 60 °C with a heating rate of 1 °C/min. In all cases, the same diffraction peaks are observed. All of them, except the peak at 1.49 $Å^{-1}$ (4.2 Å), have been attributed to a helical conformation of PEG chains for the sample of PEG 1500. Consequently, one can deduce that the PEG part of the mono- and diacyl polyoxyethylene glycols (MPEG and DPEG) will take the same helical conformation as the PEG 1500 studied previously. Moreover, the temperature dependence of these peaks is similar to those observed in SAXS for the two lamellar phases at 121 and 90 Å. Consequently, these two lamellar phases can be associated to the MPEG and the DPEG.

Finally, the large peak in WAXS at 1.49 $Å^{-1}$ (4.2 Å) can be linked by its thermal behavior to the lamellar phase observed in SAXS at 0.127 $Å^{-1}$ (49.5 Å). For these two peaks, the same temperature of crystallization ($T = 47$ °C) and melting are found (Figures 4d and 5d). Consequently, this lamellar phase observed for the Gelucire 50/13 and missing in the PEG 1500 can be ascribed to the glyceride part of the sample. Triglycerides crystallize mainly under three polymorphic forms, namely, α, β', and β. Following previous studies, in the sample such a peak at 1.49 $Å^{-1}$ (4.2 Å) can be attributed to the existence of a phase under a variety α, with the chains under a hexagonal lattice.[24−26]

C. Infrared Study. The sample was melted at 60 °C and then crystallized at 20 °C before infrared measurements. Therefore, this measurement can be compared with the second fusion of the sample obtained by X-ray diffraction (Figures 4e−f and 5e−f). Infrared spectra were recorded every 10 min from 20 °C to 55 °C at 0.3 °C/min. Figure 6 represents only several spectra, revealing the structural changes in the sample as the temperature rises up. Table 2 gives the assignment of the principal bands observed at 20 °C.

Infrared spectroscopy has been used extensively to characterize lipids[9,13] and the different conformations of PEG, helical or zigzag.[21,27] It appears clearly that several bands are temperature-dependent. As seen in a previous chapter, pure PEG adopts a helical conformation with repeating trans, trans, and gauche conformation. For such conformations, characteristic bands

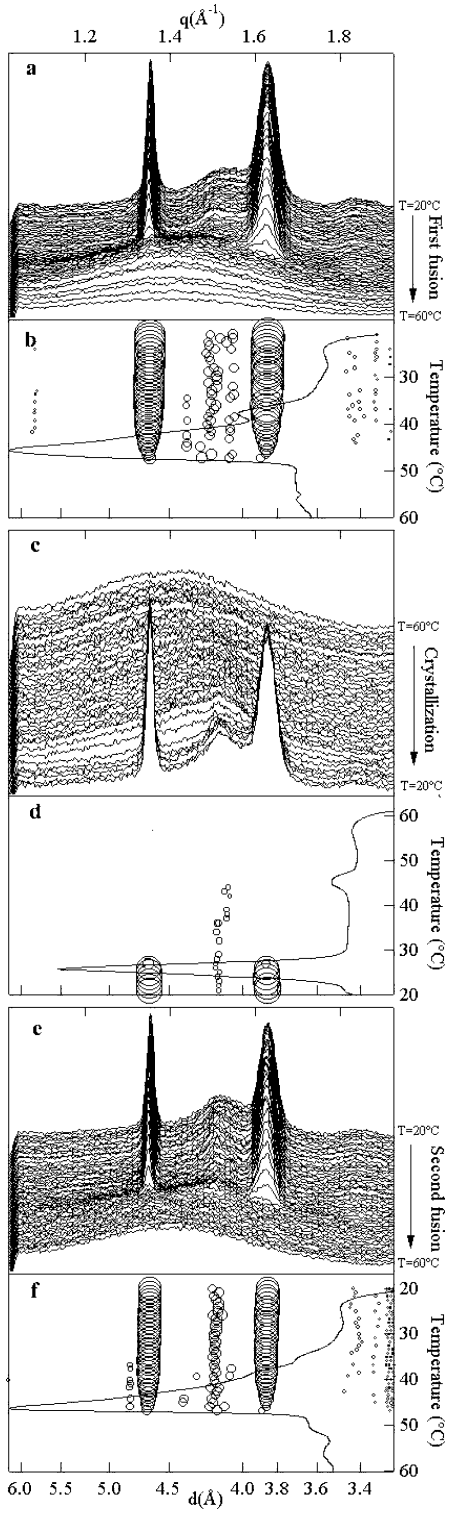

Figure 5. Evolution of WAXS patterns with the temperature for (a) the first fusion, (c) the crystallization, and (e) the second fusion of the untreated sample of Gelucire 50/13 at 1 °C/min. (b, d, f) Position and intensity (size of the symbol) of each peak observed in WAXS.

provided by the rocking modes of the methylene groups of the $O-CH_2-CH_2-O$ group are observed. These bands are clearly present at room temperature at 842 cm^{-1}, 947 cm^{-1}, 954 cm^{-1}, 1061, 1280, and 1360 cm^{-1} and completely disappear as the temperature reaches 42 °C where the sample begins to melt. It confirms X-ray patterns for which a helical conformation of PEG chains was found.

First, before 42 °C, no modification in frequency or intensity is observed except from the large structure between 2800 and

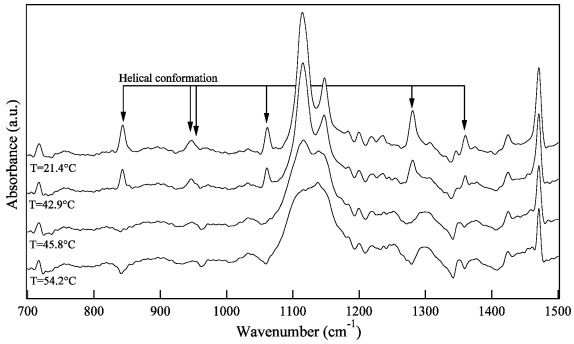

Figure 6. Mid-infrared spectra of Gelucire 50/13 melt. The bands representative of the helical conformation of the PEG chains have been marked with arrows.

TABLE 2: IR Band Positions and Assignments for Gelucire 50/13[a]

wavenumber (cm^{-1})	assignment
716	r(CH_2)
842	r(CH_2)a
947	r(CH_2)s−ν(COC)a
954	r(CH_2)s
1061	ν(COC)a + r(CH_2)s
1115−1183	ν(C−C) + ν(C−O) + r(CH_3)
1235	τ(CH_2)s τ(CH_2)a
1280	τ(CH_2)
1351	ω(CH_2)tggt
1360	ω(CH_2)gtg
1424	δ(O−CH_2)
1471	δ(CH_2)
1715−1738	ν(C═O)
2849	ν(CH_2)s
2889	ν(O−CH_2)s
2921	ν(CH_2)a
2953	ν(O−CH_2)a

[a] Vibrational band, ν; stretching, δ; bending, r; rocking, ω; wagging, τ; twisting; s, symmetric; and a, antisymmetric. The assignment is from refs 13−15, 21, and 27.

3200 cm^{-1} associated to the stretching symmetric and asymmetric of the −CH2− group where small modifications in intensity are observed.

Second, no characteristic bands of other conformations are observed. For example, a planar zigzag conformation has an all-trans conformation and gives bands at 837, 1337, or 1500 cm^{-1}. More complex conformations that alternate trans and gauche conformations give strong bands at 1012 cm^{-1} assigned to a $\delta(CH_2)$ of trans $O-CH_2-CH_2-O$ group and 1322 cm^{-1} assigned to a combination of $-CH_2-$ rocking and stretching. None of these bands are observed on our spectra implying that these two last types of conformation are definitively not present in the sample.

Therefore, we can suggest that PEG chains present a helical conformation and that no change in conformation occurs before the complete melt of the sample. This assumption is in good agreement with the X-ray diffraction experiment, and therefore we can interpret the change observed for the long period as coming from the tilt of PEG chains and not from a structural change from a helical to a zigzag conformation.

D. Structural Model. Our sample consists of a mix of mono-, di-, and triacyl glycerol (20% in weight) and mono- and diacyl polyoxyethylene glycols (72% in weight). Polymorphic properties of glycerides have already been studied by X-ray diffraction. Three polymorphs of glycerides called α, β', and β have been characterized and can be recognized by their characteristic subcell.[24−26] These studies also showed that the polymorphic

TABLE 3: Comparison of the Long Periods Obtained for a Helical of the PEG 1500, the Mono- and Diacyl Polyoxyethylene Glycols (respectively, MPEG and DPEG)

conformation	PEG 1500	MPEG	DPEG
helical	94 Å	120 Å	145 Å

properties depend on the fatty acid composition and length and the relation between the long spacing and the number of carbons in the acyl chains as a function of the polymorphic forms has been established.[7,8]

In our case, the acyl chains of the glyceride contain 16 or 18 monomers $-CH_2-$ (50% in weight of each). Consequently, glycerides under alpha variety will present the following X-ray long spacing:

$$d_{16} = 2.59*16 + 4.10 = 45.5 \text{ Å}$$

$$d_{18} = 2.59*18 + 4.10 = 50.7 \text{ Å}$$

The value of 50.7 Å for acyl chains containing 18 carbons is close to the value of 49.5 Å found in SAXS. Since the proportion of acyl chains with 18 and 16 carbons is approximately the same, then we can estimate that for steric reasons, the stearic chain, which is the longest chain, imposes the packing of the glycerides. The glycerides present in the Gelucire 50/13 form a lamellar phase with a long spacing of 49.5 Å with a hexagonal subcell noted α variety. Moreover, the persistence of this unstable variety could be attributed to the crystallization of the MPEG and DPEG part which prevents the transition to a more stable variety β or β'.

A similar analysis can be made for the MPEG and DPEG constituents of the sample representing around 72% of the sample. As already seen in previous sections, X-ray diffractograms and infrared spectra are leading to a helical conformation of the PEG chains. However, we cannot directly compare the long distance found for the PEG 1500 and those obtained for the MPEG and DPEG for which we have to take into account the acyl chain (C_{16} and C_{18}) that ends one or two parts of the PEG.

Table 3 represents the theoretical length predicted for free PEG, MPEG, and DPEG with the PEG chains under a helical conformation without tilt of the chains. The theoretical long periods for MPEG and DPEG, respectively, 120 Å and 145 Å, were evaluated by the sum of the long period of the PEG 1500 with the long period of, respectively, one and two acyl chains in C_{18}.

However, the value of 120 Å obtained for MPEG is the only value approaching that of 121 Å observed by X-ray diffraction whereas our sample is principally composed of DPEG. This value of 120 Å could be explained if the acyl chains at PEG ends interpenetrate each other and the periodic structure observed by X-ray diffraction would be the same as the MPEG (see Figure 7).

In this particular case, the surface section developed by the acyl chains may be half of the surface section developed by the PEG chain. The unit cell of PEG in helical conformation contains four helical chains, with $a = 8.05$ Å and $b = 13.04$ Å as the cell parameters. Therefore, a surface of 105 Å^2 is found for one unit cell of PEG in a helical conformation.

The sectional surface of one acyl chain ranges from 18.6 Å^2 to 20.4 Å^2 [21] depending on its polymorphic form (β, β', and α). If they interpenetrate each other, eight acyl chains are needed, and the total surface developed is ranging between 148 Å^2 and 160 Å^2, which is far from the 105 Å^2 provided by the PEG.

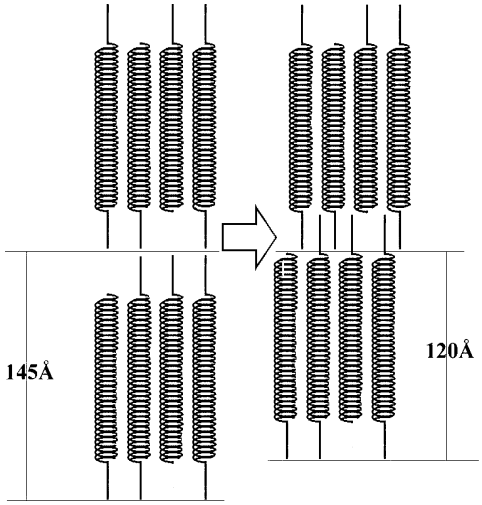

Figure 7. Schematic representation of the MPEG and DPEG with the PEG under a helical conformation and one or two acyls at the end. This drawing gives the two long periods observed before and after the acyl chains interpenetrate.

Besides, chemical analysis has shown that statistically only 72% of the PEG is ended by one acyl chain. The surface developed by the acyl chain is reduced by 28% and a theoretical value ranging from 106 to 115 Å is found, which is closer to the value of 105 Å^2 provided by the PEG. Hence, the interpenetration of the acyl chains, which ended the PEG groups, seems to be possible. Figure 7 presents a simple and schematic drawing of the possible configuration in which two acyl chains interpenetrate each other.

Nevertheless, the structure of 90 Å observed at room temperature is not explained by these previous considerations. The low level of modification of the WAXS signal when the structure at 90 Å overbalances that at 121 Å can exclude a change of conformation, helical to zigzag, for example. The SAXS behaviors of these two lamellar phases clearly indicate that these structures are in close correlation. A progressive tilt of a part (the helical chain) or of the complete molecule of MPEG and DPEG may explain such a transformation.

Previous studies[28−31] on compounds with long hydrocarbon chains have highlighted structural modifications based on the tilting of chains with respect to the short and the long side of the subcell. The tilt occurs in a stepwise fashion, carbon by carbon, giving rise to preferred conformations. Such behavior can be related to the MPEG and DPEG chains of the sample and in particular to the regular shift of the structure at 90 Å to the structure at 120 Å. To provide a more quantitative evaluation of the structural changes, the peak between 0.05 Å^{-1} and 0.07 Å^{-1} was decomposed into Gaussians allowing an accurate fit of the whole peak; the inset of Figure 8 presents an example of such mathematical treatment at $T = 39.5$ °C.

As a first step, we used a double exponential equation to fit the background and to subtract its contribution to the diffraction peak. As a second step, free fits of three Gaussians were performed on the results of the background subtraction. According to the decomposition in three Gaussians described above, for each X-ray pattern obtained between 20 °C and 45 °C, free fits of the data were performed yielding the position and the intensity of each Gaussian. These results are plotted in Figure 8. To simplify the figure, the same symbol is used for the three Gaussians and dashed lines serve as guidelines. The size of the symbol is proportional to the intensity of the peak.

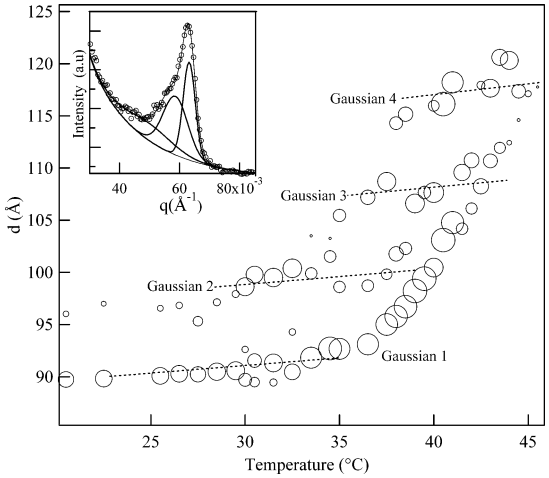

Figure 8. Evolution of each long spacing with temperature. The size of the symbol is proportional to the intensity of each peak. Inset: Decomposition into three Gaussians of the peak at 0.06 Å^{-1} provided by a sample at $T = 39.5$ °C.

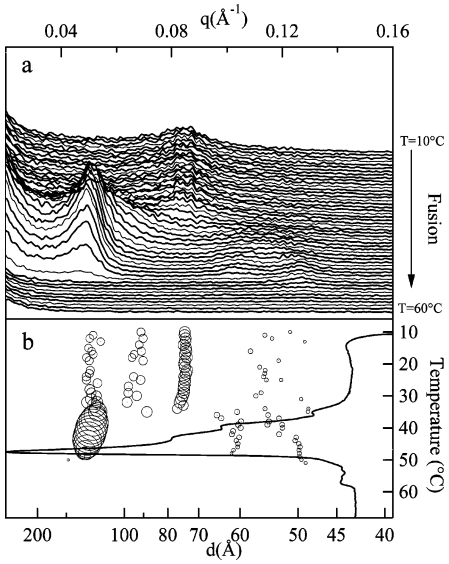

Figure 9. SAXS patterns during the fusion at 1 °C/min of the sample after quenching in liquid nitrogen.

This evolution of the Gaussians with temperature can be related to the evolution of preferential conformations of the MPEG and the DPEG:

At ambient temperature, the structure at 90 Å is predominant in proportion. As the temperature is increased, this lamellar structure disappears progressively and at $T = 30$ °C a new lamellar structure with a longer spacing (about 100 Å) is present.

At 35 °C, a third lamellar phase with an even longer period of 105 Å is formed. At this temperature, three different lamellar structures coexist (94, 99, and 105 Å).

At 40 °C, another structure of 115 Å appears, and the lamellar structure of 90 Å disappears. At $T > 43$ °C, before the complete melting of the sample, only one structure exists with a long spacing of 120 Å. This evolution toward larger distance suggests that, as the temperature is raised, the angle of the tilt is decreasing and therefore the long spacing is increased. The molecules stand up progressively and step by step.

However, we cannot attribute this tilt to a specific part of the molecule or the complete molecule. Previous works on diblock and triblock oligomers have shown that different values of tilt are possible for each block. For example, Dorset et al.[32] have shown that for a diblock compound of $CH_3(CH_2)_m-(OCH_2CH_2)_n-OH$ the alkyl chains present a tilt of 25° toward the polyoxyethylene segment.

Therefore, if we want to evaluate the conformation of the MPEG and DPEG molecule, we have to take into account the possible interpenetration of the acyl chain and the possible tilt of a part or the entire molecule. Consequently, this leads to an important number of possible conformations of the molecules in agreement with the long period observed by SAXS. A more precise evaluation of the conformation of the MPEG and DPEG molecules could be obtained by comparison with similar molecules with different lengths of hydrocarbon chain or polyoxyethylene group.[30,31]

This specific evolution is only observed during the second fusion of the sample. During the first fusion of the sample, the transition from 90 to 120 Å is direct and no other lamellar phase with intermediate spacing is observed. This phenomenon can be related to the thermal history of the sample and in particular to the conditioning in pellets. To study further the thermal evolution, we evaluate how the crystallization rate of the sample influences the structure in the following section.

E. Influence of the Crystallization Rate on the Structure. The influence of the crystallization rate on the formation of preferential conformations was analyzed to bring insight into the polymorphism of the sample. For this purpose, we compared the X-ray diffraction patterns obtained for two samples held 10 min at 80 °C and then crystallized at two different cooling rates. The first sample was quenched into liquid nitrogen, and the second one was slowly cooled to 15 °C without any thermal contribution other than the temperature of the room (final cooling rate is expected to be less than 0.1 °C/min).

Figure 9 displays the 3D evolution of SAXS pattern with the temperature during the fusion of a sample after quenching in liquid nitrogen. At room temperature, the sample is mainly in a new lamellar phase with a period of 74 Å. The two other s's of 90 and 120 Å attributed to PEG chains are also observed. When the temperature of the sample reaches 34 °C, the 74 Å and 90 Å spacings disappear in favor of the 120 Å spacing. We attribute this new lamellar phase of 74 Å to a new conformation of the MPEG and DPEG chains. Moreover, one can notice that the evolution of the X-ray pattern is close to that observed during the first fusion of the untreated sample (Figure 4a and b). In these two cases, the long spacing of the lamellar phase changes suddenly near 36 °C, passing from 90 to 120 Å within minutes, and no intermediate lamellar phases are observed as for the second fusion. In fact, for the untreated sample, which was analyzed as received (small pellets), one can deduce that the production of these pastilles is similar to the quench of the sample in liquid nitrogen. In these two cases, we favor the formation of the smaller lamellar phase 90 Å or even 74 Å to the detriment of the 120 Å lamellar phase. Because of the proximity of the peak at 74 Å and the second order of the peak at 120 and 90 Å, the visualization of the structure at 50 Å is not easy. Meanwhile, the same structure at 50 Å is clearly observed when the temperature reaches 40 °C. Interestingly, this shows that whatever the cooling rate (even very fast), it is always possible to reach the most stable form at 120 Å by heating again the excipient at 36 °C for a few minutes.

The same experiment on a sample slowly cooled (approximately 0.1 °C/min) to room temperature is presented on Figure 10. In this case, only one lamellar phase is present, with a spacing of 115 Å, even at room temperature. When the temperature reaches 40 °C, the long spacing gradually increases and reaches the value of 125 Å just before the melting of the

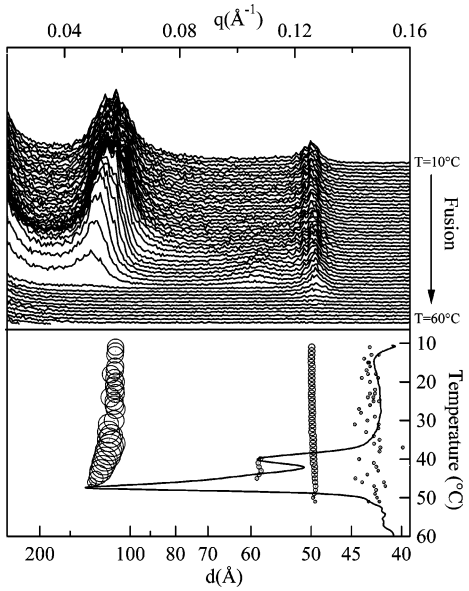

Figure 10. SAXS patterns during the fusion at 1 °C/min of a sample cooled at 0.1 °C/min.

sample at 46 °C. The peak at 50 Å of the glycerides is clearly observable and presents no modification in intensity or in position.

In brief, by cooling the sample slowly, we favor the formation of long lamellar phases of 120 Å for PEG chains sensed to form lamellar phases without tilt of the PEG chains and with interpenetration of the acyl chains ending the PEG molecules. Conversely, a rapid (1 °C per minute) or an abrupt cooling will favor the formation of polymorphic form with a smaller long period, 90 Å or even 74 Å. The structure of the associated glyceride phase does not seem to be influenced by the crystallization rate and always forms a lamellar phase of 50 Å with a hexagonal subcell.

IV. Conclusion

The combination of infrared spectroscopy and X-ray diffraction at both small and wide angle coupled to DSC has enabled to characterize all the polymorphs, and their thermal behaviors, present in PEG 1500 and Gelucire 50/13.

PEG 1500 crystallizes in a slightly distorted helical structure noted (7/2) helix under an orthorhombic subcell unlike structural studies on PEG presenting a higher molecular weight where a monoclinic subcell is generally observed. In the present structure (orthorhombic subcell), a lamellar phase with a longer spacing of 96.7 Å has been evidenced by small-angle X-ray diffraction.

Gelucire 50/13, which consists of a mix of glycerides and mono- and diacyl polyoxyethylene glycol, presents a complex structure which is dependent on its thermal history. Several lamellar phases at 74 Å, 90 Å, 99 Å, 106 Å, and 120 Å have been highlighted for the mono- and diacyl polyoxyethylene glycol depending on the thermal history and, in particular, the crystallization rate of the sample. This increase of the long period and the low level of modification of the WAXS signal can exclude a change of conformation but may be provided by a progressive tilt of a part (the helical chain) or of the complete molecule of MPEG and DPEG. This tilting may be combined with the interpenetration of the acyl chains, which end one or two parts of the PEG chains.

A mathematical treatment of the diffraction peaks observed during the second fusion of the sample, particularly when the structure at 90 Å overbalances that at 121 Å, has shown the presence of intermediate lamellar phases of 99 and 106 Å. This regular increase of the long period occurring in a stepwise fashion with the temperature can be link to the decrease of the tilt of the molecule as already observed on compounds with long hydrocarbon chains.

Some parameters are found independent of the thermal history, however. The glyceride part of the sample in all cases forms a lamellar phase with a long period of 49.5 Å under the variety alpha or the hydrocarbon chains under a hexagonal lattice. Moreover, the X-ray diffractograms and infrared spectra led to a helical conformation of the PEG chains of the mono- and diacyl polyoxyethylene glycol whatever the thermal treatment of the sample.

By coupling X-ray diffraction and DSC, the thermal behavior has been established. For each lamellar phase, the thermal treatment was characterized, leading to the formation of these lamellar phases. It reveals that a slow cooling rate favors the formation of a unique lamellar phase of 120 Å having the higher melting point, whereas a rapid cooling rate produces polymorphic lamellar phases with a long period of 74, 90, and 120 Å. However, heating the excipient at 36 °C for a few minutes allows the formation of the 120 Å lamellar phase. Nevertheless, the nature and value of the tilt of mono- and diacyl polyoxyethylene glycol remain uncertain.

Structural studies by X-ray diffraction on pure mono- or diacyl polyoxyethylene glycol and molecular simulation may provide some information on these structures. Moreover, as performed in the work of Booth and Price,[30,31] comparison with similar molecules with different lengths of hydrocarbon chains or polyoxyethylene groups should give a more precise evaluation of the conformation of the MPEG and DPEG molecules. In term, the description of the polymorphism of this family of excipient is of great importance for pharmaceutical science as it is linked to excipient structure control and drug release. These excipients are not necessarily pure compounds but mixtures accepted for many decades by pharmacopoeias. Then, the number of authorized mixtures is limited and they should be characterized as they are produced.

References and Notes

(1) Sutananta, W.; Craig, D. Q. M. *J. Pharm. Pharmacol.* **1995**, *47*, 182−187.

(2) Damian, F.; Blaton, N.; Kinget, R.; Van de Mooter, G. *Int. J. Pharm.* **2002**, *244*, 87−98.

(3) Vippagunta, S. R.; Maul, K. A.; Tallavajhala, S.; Grant, D. J. W. *Int. J. Pharm.* **2002**, *236*, 111−123.

(4) Sutananta, W.; Craig, D. Q. M.; Newton, J. M. *Int. J. Pharm.* **1994**, *111*, 51−62.

(5) Takahashi, Y.; Tadokoro, H. *Macromolecules* **1973**, *6*, *5*, 672−675.

(6) Russell, T. P.; Ito, H. *Macromolecules* **1988**, *21*, 1703−1709.

(7) Garti, N.; Sato, K. In *Crystallization and polymorphism of fats and fatty acids*; New York, 1988; pp 97−138.

(8) Small, D. M. In *Handbook of Lipid Research 4, The Physical Chemistry of Lipids, From alkanes to Phospholipids*; Plenum Press: New York and London, 1986; pp 345−394, 4.

(9) Yano, J.; Kaneko, F.; Kobayashi, M.; K. Sato *J. Phys. Chem. B* **1997**, *101*, 8112−8119.

(10) Neyertz, S.; Brown, D.; Thomas, J. O. *J. Chem. Phys.* **1994**, *101*, *11*, 10064.

(11) Johnson, J. A.; Saboung, M. L.; Price, D. L.; Ansell, S. *J. Chem. Phys.* **1998**, *109*, *16*, 7005−7010.

(12) Keller, G.; Lavigne, F.; Forte, L.; Andrieux, K.; Dahim, M.; Loisel, C.; Ollivon, M.; Bourgaux, C.; Lesieur, P. *J. Therm. Anal. Calorimetry* **1998**, *51*(*3*), 738−791.

(13) Chapman, D. In *The structure of lipids by spectroscopic and X-ray techniques*; Methuen and co ltd: London, 1965.

(14) Papke, B. L.; Ratner, M. A.; Shriver, D. F. *J. Phys. Chem. Solids* **1981**, *42*, 493.

(15) Nazar, L. F.; Wu, H.; Power, W. P. *J. Mater. Chem.* **1995**, *5*, 1985−1993.

(16) Roy, P.; Mathis, Y.-L.; Lupi, S.; Nucara, A.; Tremblay, B.; Gerschel, A. *Synchrotron Radiation News* **1995**, 5, *415*, 8.

(17) Roy, P.; Mathis, Y.-L.; Paolone, A.; Giura, P.; Nucara, A.; Lupi, S.; Calvany, P.; Gerschel, A. *Nuovo Cimento Soc. Ital. Fis.* **1998**, *415*, 20D.

(18) Mathis, Y.-L.; Roy, P.; Tremblay, B.; Nucara, A.; Lupi, S.; Calvani, P.; Gerschel, A. *Phys. Rev. Lett.* **1998**, *3*, *1220*, 80.

(19) Lee, S. W.; Chen, E.; Zhang, A.; Yoon, Y.; Moon, B. S.; Lee, S.; Harris, F. W.; Cheng, S. Z. D. *Macromolecules* **1996**, *29*, *27*, 8816−8823.

(20) Chen, E. Q.; Lee, S. W.; Zhang, A.; Moon, B. S.; Mann, I.; Harris, F. W.; Cheng, S. Z. D. *Macromolecules* **1999**, *32*, *15*, 4784−4793.

(21) Evans, C. C.; Bates, F. S.; Ward, M. D. *Chem. Mater.* **2000**, *12*, *5*, 236−249.

(22) Takahashi, Y.; Sumita, I.; Tadokoro, H. *J. Polym. Sci.* **1973**, *11*, 2113−2122.

(23) Tadokoro, H.; Chatani, Y.; Yoshihara, T.; Tahara, S.; Murahashi, S. *Makromol. Chem.* **1964**, *73*, 109.

(24) Larsson K. *Acta Chem. Scand.* **1966**, *20*, 2255−2260.

(25) Hoerr, C. W.; Paulicka, F. R. *J. Am. Oil Chem. Soc.* **1968**, *45*, 793.

(26) Vand, V.; Bell, I. P. *Acta Crystallogr.* **1951**, *4*, 465.

(27) Jeevanandam, P.; Vasudevan, S. *Chem. Mater.* **1998**, *10*, *5*, 1276−1285.

(28) Small, D. M. In *Handbook of Lipid Research 4, The Physical Chemistry of Lipids, From alkanes to Phospholipids;* Plenum Press: New York and London, 1986; pp 233−285, 4.

(29) Precht, D. *Kiel. Milchwirtsch. Forschungsber* **1974**, *26*, 221.

(30) Mai, S. M.; Fairclough, J. P. A.; Terrill, N. J.; Turner, S. C.; Hamley, I. W.; Matsen, M. W.; Ryan, A. J.; Booth, C. *Macromolecules* **1998**, *31*, *23*, 8110−8116.

(31) Hamley, I. W.; Castelletto, V.; Yang, Z.; Price, C.; Booth, C. *Macromolecules* **2001**, *34*, *12*, 4079−4081.

(32) Dorset, D. L. *J. Colloid Interface Sci.* **1983**, *96*, 172−181.